Journal of Alloys and Compounds 509 (2011) 3509–3514

Contents lists available at ScienceDirect

Journal of Alloys and Compounds

journal homepage: www.elsevier.com/locate/jallcom

# Interfacial reactions between high-Pb solders and Ag

Chi-Pu Lin [a], Chih-Ming Chen [a,*], Yee-Wen Yen [b], Hsin-Jay Wu [c], Sinn-Wen Chen [c]

[a] Department of Chemical Engineering, National Chung Hsing University, Taichung 402, Taiwan
[b] Department of Materials Science and Engineering, National Taiwan University of Science and Technology, Taipei 106, Taiwan
[c] Department of Chemical Engineering, National Tsing Hua University, Hsinchu 30043, Taiwan

ARTICLE INFO

*Article history:*
Received 15 October 2010
Received in revised form
13 December 2010
Accepted 16 December 2010
Available online 24 December 2010

*Keywords:*
Intermetallics
Metals and alloys
Liquid–solid reactions
Diffusion
Microstructure

ABSTRACT

Interfacial reactions between high-Pb solders (Pb–10Sn, Pb–5Sn, and Pb–3Sn, in wt.%) and immersion Ag layer at 350 °C are investigated. Upon decreasing the Sn concentration from 10 wt.% to 5 wt.%, the reaction product formed at the solder/Ag interface changes from the $Ag_3Sn$ phase to the $Ag_4Sn$ phase. When the Sn concentration reduces to only 3 wt.%, the reaction product is the $Ag_4Sn$ phase at the initial stage of reaction but transforms to the (Ag) phase dissolved with Sn at the later stage of reaction. Pb penetrates across the (Ag) phase via grain boundary and forms a continuous Pb-rich layer between the (Ag) phase and the bottom Cu layer. The correlation between the phase transformation and the solder composition is discussed based on the calculated Sn–Pb–Ag isothermal section.



## 1. Introduction

Development of lead (Pb)-free solders is an urgent issue in the electronic packaging industries due to the concerns of Pb toxicity on the environment and human health [1]. Tin–silver–copper (SnAgCu)-based solders are currently the representatives of the Pb-free solders used for consumer electronics [2,3]. However, the SnAgCu-based solders are not qualified for some specific applications, like high-end microprocessors, because the melting point (~217 °C) is not high enough that can withstand high-temperature operation environment and multiple reflow conditions. High-Pb solders with a Pb content higher than 90 wt.% possess higher melting point (~300 °C) and have been used as the high temperature solders for a long period of time [4,5]. Although efforts have been made to develop high-temperature Pb-free solders like gold–tin, tin–zinc, and bismuth–silver alloys, none of them is fully comparable to the high-Pb solders [6–10]. Therefore, the development of high-temperature Pb-free solders remains a challenge and an incomplete task. At present, the high-Pb solders are still the most reliable high-temperature solders for practical applications.

To fabricate the solder joints, the high-Pb solders are joined with the metallization layers by means of a reflow process. During reflow, the high-Pb solders melt and wet the metallization layers. Interfacial reactions usually take place and then the joining completes. Understanding the interfacial reactions between solders and metallization layers is helpful to gain reliable solder joints. Copper (Cu) and nickel (Ni) are two common metallization layers and their interfacial reactions with high-Pb solders have been investigated [11–15]. Different from those in the cases of eutectic SnPb and Pb-free solders, only one intermetallic compound, $Cu_3Sn$, was formed in the interfacial reaction between 95Pb5Sn (in wt.%) solder and Cu-based metallization layers [16–18]. The $Cu_3Sn$ compound even spalled off the underlying Cu metallization after long-term solid-state annealing [11]. These unusual phenomena were attributed to the insufficient supply of Sn in the high-Pb solders for the interfacial reaction. For another Ni metallization, when the 99Pb1Sn solder was reflowed on an electroless Ni(P) layer, the $Ni_3Sn_2$ phase was formed first at the solder/Ni(P) interface, followed by the formation of the $Ni_3Sn$ phase at the $Ni_3Sn_2$/Ni(P) interface [16,19]. As the Sn content in solder increased to 5 wt.% (95Pb5Sn), the $Ni_3Sn_2$ phase was formed first as well, but the $Ni_3Sn_4$ phase instead of the $Ni_3Sn$ phase was the intermetallic compound next formed [20]. Spalling of the $Ni_3Sn_4$ compound off the underlying Ni metallization was also observed after long-term reflow [12,15].

Ag is also a common metallization used for electronic packaging, such as the immersion Ag used for the surface finish layer [21–23]. However, to the best of our knowledge, the interfacial reactions between the high-Pb solders and Ag are not yet reported in the literatures. This present study investigates the interfacial reactions of three high-Pb solders (90Pb10Sn, 95Pb5Sn,and 97Pb3Sn, all in wt.%) and Ag reflowed at 350 °C. In general, typical reflow soldering

* Corresponding author. Tel.: +886 4 22859458; fax: +886 4 22854734.
*E-mail addresses:* chencm@nchu.edu.tw, chencm@dragon.nchu.edu.tw (C.-M. Chen).

0925-8388/$ – see front matter © 2010 Elsevier B.V. All rights reserved.
doi:10.1016/j.jallcom.2010.12.135

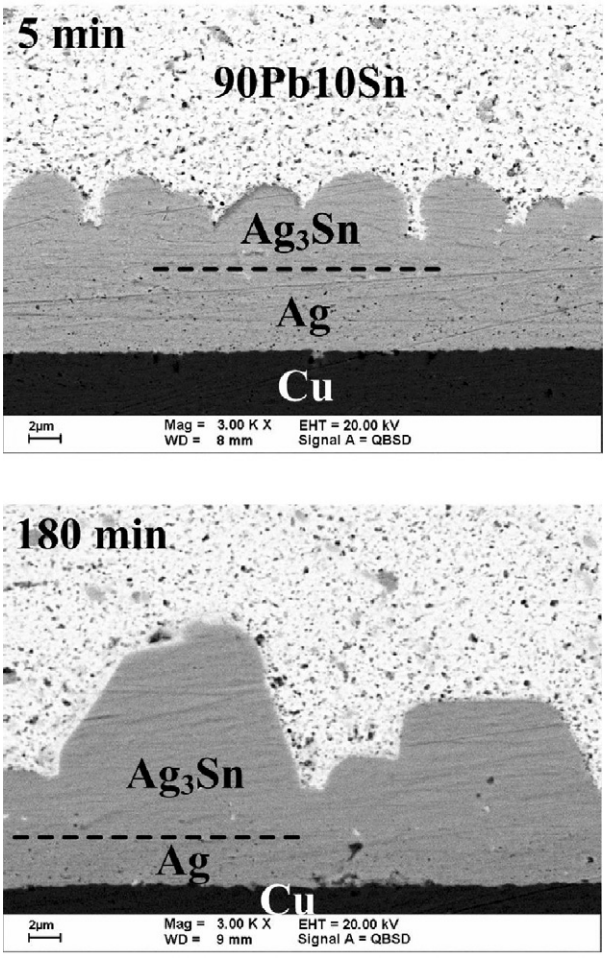


**Fig. 1.** SEM micrographs showing the cross-sectional microstructures of the 90Pb10Sn/Ag interfaces reacted at 350 °C for (a) 5 min and (b) 180 min.

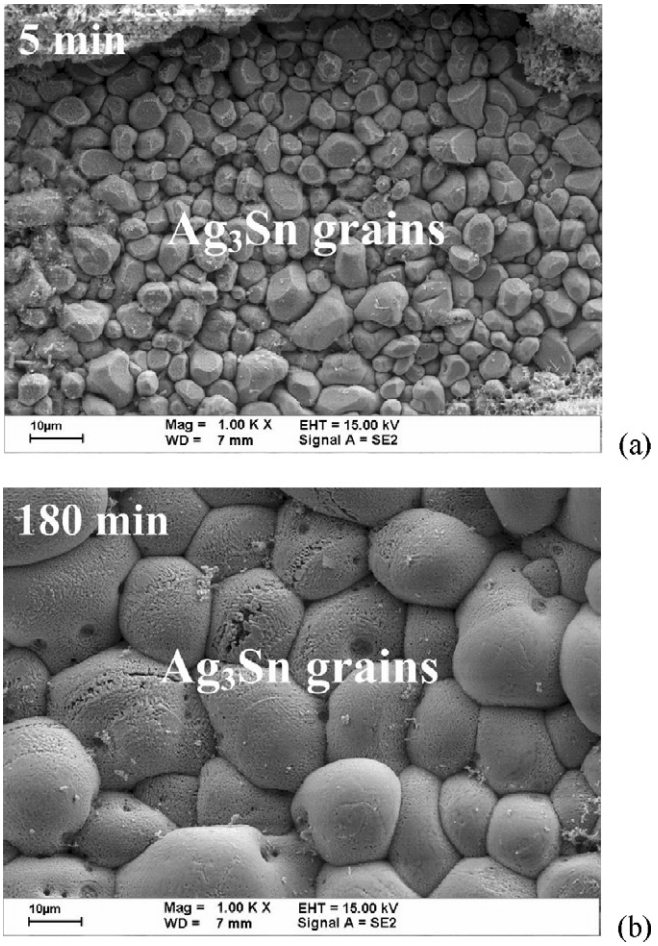


**Fig. 2.** Top-view SEM micrographs of the $Ag_3Sn$ grains formed at the 90Pb10Sn/Ag interfaces reacted at 350 °C for (a) 5 min and (b) 180 min.

takes only a few minutes. In this present study, we performed the reflow experiments from 5 min to 180 min to gain a better understanding of the interfacial reaction of the high-Pb solder with Ag. Formation of intermetallic compounds and morphological evolution at the solder/Ag interface were examined.

## 2. Experimental

A Ta/Cu bilayer was deposited on an oxidized Si substrate using electron beam evaporation, where the thicknesses of Ta and Cu were 200 Å and 4000 Å, respectively. The Ta/Cu bilayer was then patterned to a square pad with a dimension of 600 μm × 600 μm using photolithography technique. Using the electroplating technique, the Cu layer was grown to 10 μm thick. An immersion Ag layer of 10 μm thickness was deposited on the Cu layer by immersing the Si substrate in a commercial plating solution at 58 °C. Solder alloys of three different compositions, 97Pb3Sn, 95Pb5Sn, and 90Pb10Sn, were prepared. Proper amounts of Sn and Pb shots, both 99.99% purity, were weighted and sealed in a vacuum ($2.3 \times 10^{-2}$ Torr) quartz tube. The quartz tube was then put into a furnace at 500 °C to make the Sn and Pb shots melt and mix together. After 72 h, the quartz tube was removed from the furnace and quenched in ice water. A small piece of solder (~0.16 mg) was cut from the solidified ingot. The solder piece was cleaned and then placed on the flux-coated (rosin mildly activated (RMA) flux) Ag immersion layer. The reflow reaction was conducted by placing the sample on a 350 °C hot plate for 5–180 min.

After the predetermined reflow durations, the samples were removed from the hot plate and treated by metallographic examinations. The samples were mounted in epoxy resin, followed by grinding and polishing with sandpapers and fine $Al_2O_3$ powders in the direction perpendicular to the solder/Ag interface. For clear observation, some samples were dipped into an etching solution of 95 vol.% $CH_3OH$ and 5 vol.% HCl for a few seconds to remove the solder portion. A scanning electron microscope (SEM) was used to observe the microstructure of the solder/Ag interface. The composition analysis was carried out using a field-emission electron probe microanalyzer (FE-EPMA).

## 3. Results and discussion

### 3.1. Interfacial reaction between 90Pb10Sn solder and Ag

Fig. 1(a) and (b) shows the cross-sectional microstructures in backscattered electron mode of the 90Pb10Sn/Ag interface reacted at 350 °C for 5 and 180 min, respectively. The only intermetallic compound formed at the interface after reaction for 5 min was scallop-shaped and was identified as the $Ag_3Sn$ phase according to the EPMA analysis (24.14 at.% Sn–75.86 at.% Ag). When the reaction was extended to 180 min, coarsening of the $Ag_3Sn$ phase was found as seen in Fig. 1(b). In order to observe the morphological change of the $Ag_3Sn$ phase during reaction, the solder portion was totally removed by etching to expose the surface of the $Ag_3Sn$ phase, as seen in Fig. 2(a) and (b). The $Ag_3Sn$ grains attached to each other very densely, and they coarsened with increasing the reaction time, resulting in an increase in the grain size but a decrease in the grain number. From a thermodynamic viewpoint, the occurrence of phase coarsening is to reduce the total amount of the interfacial areas, so that the total interfacial energy can be minimized.

### 3.2. Interfacial reaction between 95Pb5Sn solder and Ag

Fig. 3(a)–(d) shows the cross-sectional microstructures in backscattered electron mode of the 95Pb5Sn/Ag interface reacted at 350 °C for 5–120 min. There was only intermetallic compound formed at the interface. EPMA analysis revealed its composition was 19.53 at.% Sn–80.47 at.% Ag, which was identified as the

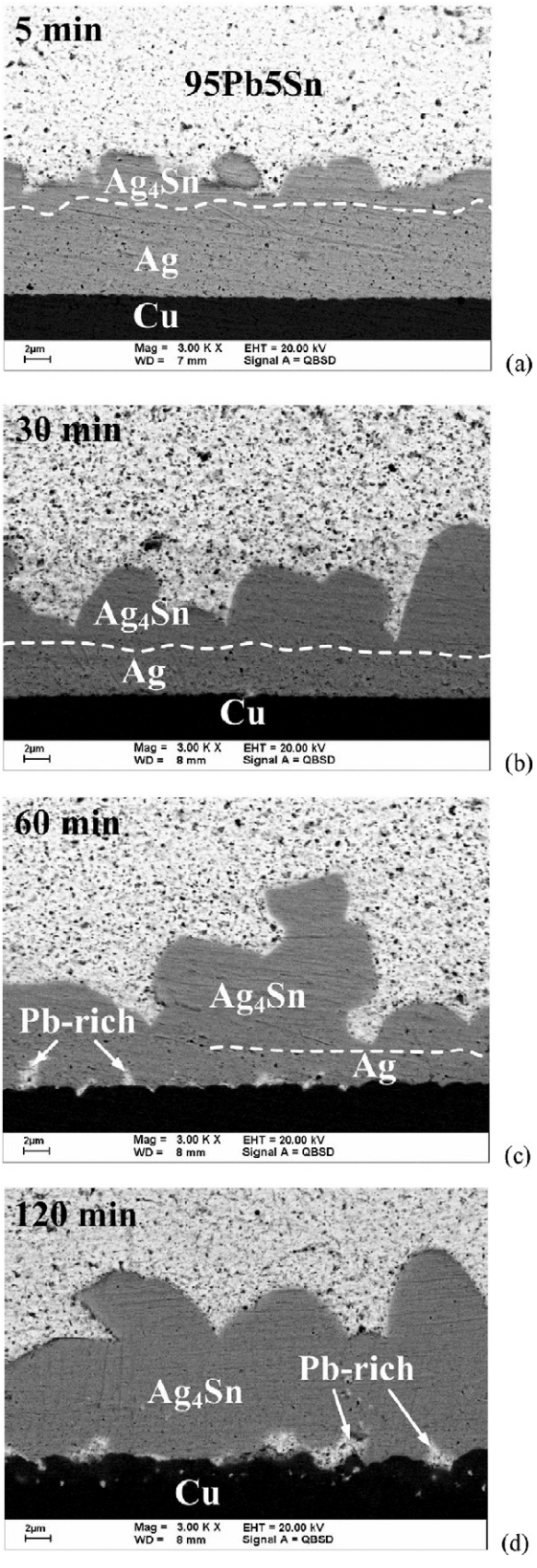


**Fig. 3.** SEM micrographs showing the cross-sectional microstructures of the 95Pb5Sn/Ag interfaces reacted at 350 °C for (a) 5 min, (b) 30 min, (c) 60 min and (d) 120 min.

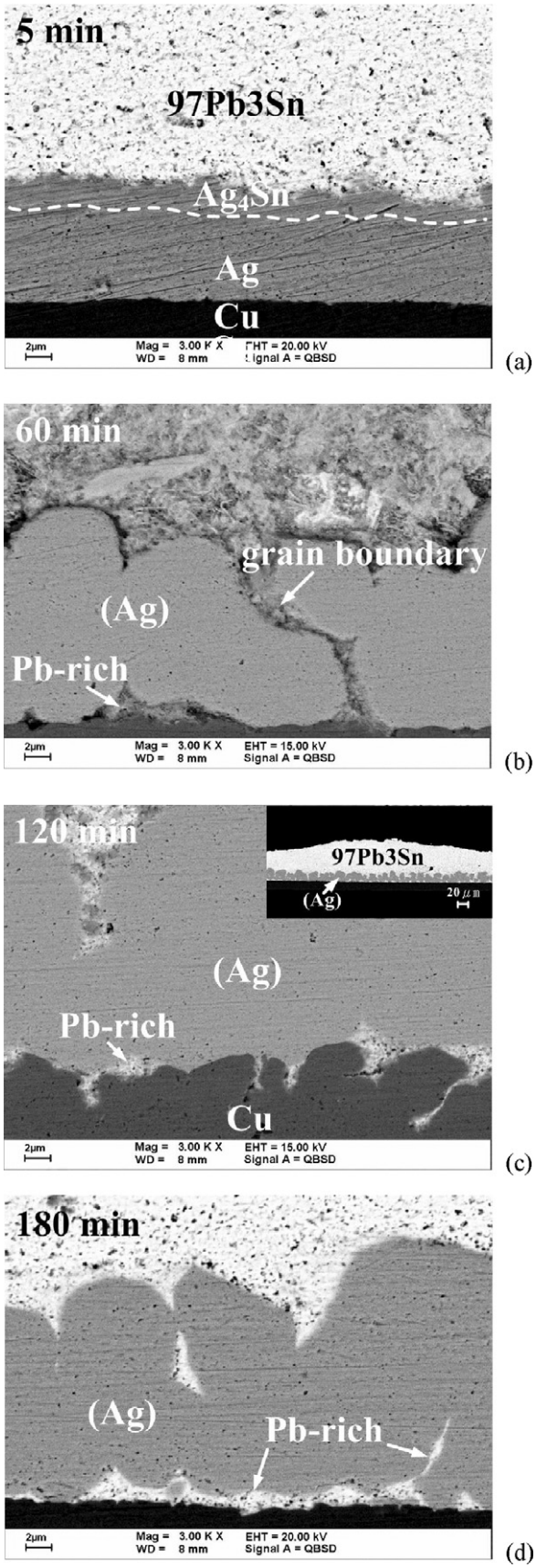


**Fig. 4.** SEM micrographs showing the cross-sectional microstructures of the 97Pb3Sn/Ag interfaces reacted at 350 °C for (a) 5 min, (b) 60 min, (c) 120 min and (d) 180 min.

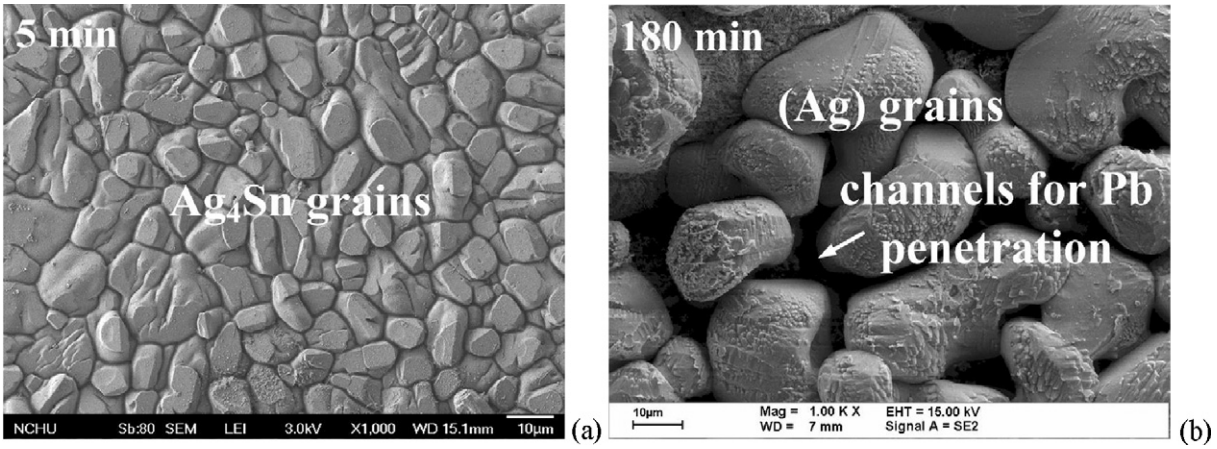


**Fig. 5.** Top-view SEM micrographs of the $Ag_4Sn$ grains formed at the 97Pb3Sn/Ag interfaces reacted at 350 °C for (a) 5 min and (b) 180 min.

$Ag_4Sn$ phase. Similar to the above-mentioned $Ag_3Sn$ phase at the 90Pb10Sn/Ag interface, coarsening of the $Ag_4Sn$ phase was also observed with increasing the reaction time. When the reaction was prolonged to 60 min, the solder/$Ag_4Sn$ interface became very irregular and the Ag/Cu interface appeared to be filled by other substance. According to the EPMA analysis, this gray substance was the Pb-rich phase dissolved with small amounts of Sn and Ag. Due to the Pb-rich phase penetration, the Ag and Cu layers partially dissolved. Extending the reaction to 120 min, the Ag layer was completely consumed to form the $Ag_4Sn$ phase with a composition of 13.5 at.% Sn–86.5 at.% Ag. More Pb-rich phase penetrated into the $Ag_4Sn$/Cu interface.

### 3.3. Interfacial reaction between 97Pb3Sn solder and Ag

Fig. 4(a)–(d) shows the cross-sectional microstructures in backscattered electron mode of the 97Pb3Sn/Ag interface reacted at 350 °C for 5–180 min. Similar to the 95Pb5Sn/Ag interfacial reaction, the $Ag_4Sn$ phase was the only intermetallic compound formed at the 97Pb3Sn/Ag interface after reaction for only 5 min, as seen in Fig. 4(a). When the reaction time reached 60 min, it was surprising that the $Ag_4Sn$ phase disappeared but only the (Ag) phase (94.7 at.% Ag–5.3 at.% Sn) existed at the interface, as seen in Fig. 4(b). The identification of the (Ag) phase is based on its composition and the binary Sn–Ag phase diagram [24]. According to the phase diagram,

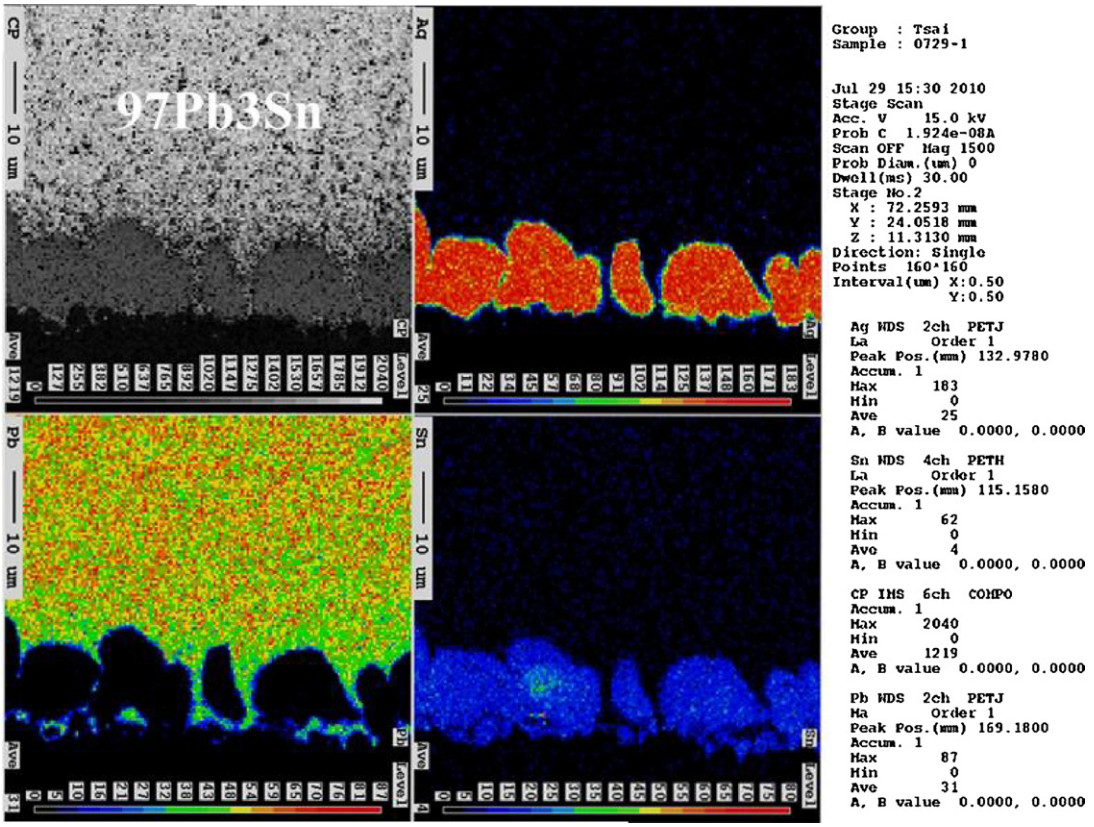


**Fig. 6.** Element mapping of EPMA of the 97Pb3Sn/Ag interface reacted at 350 °C for 90 min.

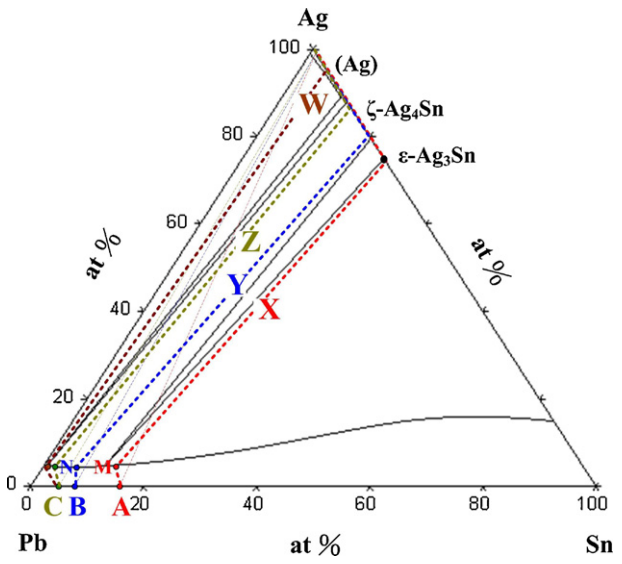


**Fig. 7.** Calculated isothermal section of ternary Sn–Pb–Ag system at 350 °C.

the (Ag) phase (solid solution) can dissolve with Sn up to 10 at.% at 350 °C. Therefore, the detected composition is referred to the (Ag) phase. It seemed that the $Ag_4Sn$ phase underwent a phase transformation and transformed to the (Ag) phase. The Pb-rich phase penetration into the (Ag)/Cu interface was also observed. Owing to etching, a grain boundary across the entire (Ag) layer was clearly seen, and was very likely to be the channel for the Pb penetration. The Pb-rich phase penetration became more pronounced after reaction for 120 and 180 min, as seen in Fig. 4(c) and (d), resulting in the spalling of the (Ag) layer off the Cu substrate. A low magnification micrograph inserted in Fig. 4(c) showed that the spalling of the (Ag) layer off the Cu substrate took place across the entire interface.

Fig. 5(a) and (b) shows the top-view microstructures of the interfaces with the solder portion totally removed. It was found that the $Ag_4Sn$ grains attached to each other very closely after reaction for 5 min. However, after reaction for 180 min, the attachment among the (Ag) grains was not as close as that among the $Ag_4Sn$ grains. Therefore, many channels were formed among the (Ag) grains for the Pb penetration from the solder side to the Ag/Cu interface.

In order to make sure only the (Ag) phase existed at the interface after long-term reaction and no any other intermetallic compound coexisted with it, the EPMA element mapping of the (Ag) phase was conducted and the result was shown in Fig. 6. It was clear that the Ag and Sn distribution in the (Ag) phase were very uniform, confirming it was indeed the (Ag) phase dissolved with Sn. Additionally, no other intermetallic compound was observed, indicating that the initially formed $Ag_4Sn$ phase had transformed to the (Ag) phase. From the element mapping of Pb, the Pb penetration through the grain boundary was clearly observed.

### *3.4. Phase transformation at the interface due to the change of solder composition*

Based on the above results, the solder concentration plays an important role in the type of the reaction product formed in the molten high-Pb solder/Ag interfacial reaction. When the Sn concentration is 10 wt.%, only the $Ag_3Sn$ phase was formed at the interface (see Fig. 1). When the Sn concentration decreases to 5 wt.%, the intermetallic compound formed at the interface transformed into the $Ag_4Sn$ phase (see Fig. 3). With only 3 wt.% Sn concentration, the $Ag_4Sn$ phase was formed first at the interface but eventually transformed into the (Ag) phase after longer reaction (see Fig. 4). To rationalize the phase transformation due to the solder concentration change, the equilibrium phase diagram is a useful tool. However, the Sn–Pb–Ag isothermal section obtained experimentally at 350 °C is not available in the literatures. So, a Sn–Pb–Ag isothermal section at 350 °C, as shown in Fig. 7, calculated by a commercial software Pandat [25–28] is employed. The point "A" (in at.%) shows the composition of the 90Pb10Sn (in wt.%) solder. Linking point "A" to the Ag phase is the mass balance line. Because the $Ag_3Sn$ phase is formed at the 90Pb10Sn/Ag interface as mentioned above, the diffusion path can be drawn as the line "X" and is 90Pb10Sn/$Ag_3Sn$/Ag. It shows that a tie-line is built up between the molten solder (dissolved with about 5 at.% Ag, as marked by the point "M") and the $Ag_3Sn$ phase, which also confirms that the $Ag_3Sn$ phase is an equilibrium reaction product at the interface. When the solder concentration decreases to 95Pb5Sn, as marked by the point "B", a possible diffusion path is drawn as the line "Y". At this moment, the solder concentration adjacent to the interface shifts from "M" to "N", and is in equilibrium with the $Ag_4Sn$ phase by a tie line. Therefore, the $Ag_4Sn$ phase is the equilibrium reaction product at the interface, which is in good agreement with the experimental results. The point "C" indicates the composition of 97Pb3Sn, and its corresponding diffusion path is drawn as the line "Z". The $Ag_4Sn$ phase is thus also the equilibrium reaction product at the interface, which is in good agreement with the experimental result of early stage of reaction, as seen in Fig. 4(a). However, very interestingly, the $Ag_4Sn$ phase disappeared after longer reaction time but the (Ag) phase appeared at the interface instead, as seen in Fig. 4(b)–(d). This remarkable phase transformation is attributed to the change of the solder composition due to interfacial reaction. Strictly speaking, it is a combined effect of the solder composition and solder amount. Because the 97Pb3Sn solder contains less Sn and the solder amount (~0.16 mg) is limited, the Sn content of solder decreases at a faster rate due to the formation of the $Ag_4Sn$ phase at the interface. Based on the EPMA analysis, the solder composition very close to the solder/$Ag_4Sn$ interface was 0.15 at.% Sn–6.65 at.% Ag–93.2 at.% Pb with nearly negligible Sn concentration after 90 min of reaction. The consumption of Sn in the solder makes the diffusion path to shift to the line "W", where the solder is in equilibrium with only the (Ag) phase. Therefore, the initially formed $Ag_4Sn$ phase transformed into the (Ag) phase as experimentally observed.

## 4. Conclusions

The interfacial reactions between molten high-Pb solders and Ag at 350 °C are significantly affected by the solder composition. The $Ag_3Sn$ phase is formed at the molten solder/Ag interface when the Sn concentration of the solder is 10 wt.%. When the Sn concentration of the solder decreases to 5 wt.%, the reaction product becomes the $Ag_4Sn$ phase. When the Sn concentration of the solder is only 3 wt.%, the $Ag_4Sn$ phase is also formed first, but it disappears and the entire Ag layer converts to the (Ag) phase dissolved with Sn with increasing the reaction time. The Pb penetration through the grain boundary of the (Ag) phase occurs and the (Ag)/Cu interface is replaced by the (Ag)/Pb-rich/Cu interface. Due to the Pb penetration, the (Ag) layer spalls off the Cu substrate. The phase transformation due to the change of the solder composition is well explained by the calculated Sn–Pb–Ag isothermal section.

## Acknowledgements

The authors gratefully acknowledge the financial support of the National Science Council of Taiwan under grants NSC 96-2221-E-005-064-MY3 and NSC 99-2628-E-005-006. This work is supported in part by the Ministry of Education, Taiwan, ROC under the ATU plan.

## References


[1] M. Abtew, G. Selvaduray, Mater. Sci. Eng. R 27 (2000) 95–141.
[2] K. Zeng, K.N. Tu, Mater. Sci. Eng. R 38 (2002) 55–105.
[3] D. Li, C. Liu, P.P. Conway, Mater. Sci. Eng. A 391 (2005) 95–103.
[4] L.F. Miller, IBM J. Res. Dev. 13 (1969) 239–250.
[5] P.A. Totta, R.P. Sopher, IBM J. Res. Dev. 13 (1969) 226–238.
[6] M. Rettenmayr, P. Lambracht, B. Kempf, C. Tschudin, J. Electron. Mater. 31 (2002) 278–285.
[7] J.N. Lalena, N.F. Dean, M.W. Weister, J. Electron. Mater. 31 (2002) 1244–1249.
[8] T. Shimizu, H. Ishikawa, I. Ohnuma, K. Ishida, J. Electron. Mater. 28 (1999) 1172–1175.
[9] J.M. Song, H.Y. Chuang, Z.M. Wu, J. Electron. Mater. 35 (2006) 1041–1049.
[10] K. Suganuma, S.J. Kim, K.S. Kim, JOM 61 (2009) 64–71.
[11] J.W. Jang, L.N. Ramanathan, J.K. Lin, D.R. Frear, J. Appl. Phys. 95 (2004) 8286–8289.
[12] K.Z. Wang, C.M. Chen, J. Electron. Mater. 34 (2005) 1543–1549.
[13] C.M. Chen, K.J. Wang, K.C. Chen, J. Alloys Compd. 432 (2007) 122–128.
[14] M.H. Tsai, Y.W. Lin, H.Y. Chuang, C.R. Kao, J. Mater. Res. 24 (2009) 3407–3411.
[15] M.H. Tsai, W.M. Chen, M.Y. Tsai, C.R. Kao, J. Alloys Compd. 504 (2010) 341–344.
[16] K.N. Tu, K. Zeng, Mater. Sci. Eng. R 34 (2001) 1–58.
[17] G.Z. Pan, A.A. Liu, H.K. Kim, K.N. Tu, P.A. Totta, Appl. Phys. Lett. 71 (1997) 2946–2948.
[18] J.W. Jang, P.G. Kim, K.N. Tu, M. Lee, J. Mater. Res. 14 (1999) 3895–3900.
[19] M. Inaba, K. Yamakawa, N. Iwase, IEEE Trans. Comp. Hyb. Manuf. Technol. 13 (1990) 119.
[20] K.L. Lin, J.M. Jang, Mater. Chem. Phys. 38 (1994) 33–41.
[21] C.P. Lin, C.M. Chen, C.H. Lin, W.C. Su, J. Alloys Compd. 502 (2010) L17–L19.
[22] C.P. Lin, C.M. Chen, J. Electron. Mater. 38 (2009) 908–914.
[23] J.L. Fang, Surf. Technol. 34 (2005) 1–5.
[24] I. Karakaya, W.T. Thompson, Binary Alloy Phase Diagrams, 2nd ed., ASM International, Materials Park, OH, 1990, pp. 94.
[25] Pandat, CompuTherm LLC, 437 S. Yellowstone Dr., Suite 217, Madison, WI 53719.
[26] W. Gierlotka, Y.C. Huang, S.W. Chen, Metall. Mater. Trans. A 39A (2008) 3199–3209.
[27] H.J. Fecht, M.X. Zhang, Y.A. Chang, J.H. Perepezko, Metall. Trans. 20 (1989) 795–803.
[28] F.H. Hayes, H.L. Lukas, G. Effenberg, G. Petzow, Z. Metall. 77 (1986) 749–754.